EUKARYOTIC CELL, Apr. 2007, p. 664–673 Vol. 6, No. 4
1535-9778/07/$08.00+0 doi:10.1128/EC.00308-06

The 29-Kilodalton Thiol-Dependent Peroxidase of *Entamoeba histolytica* Is a Factor Involved in Pathogenesis and Survival of the Parasite during Oxidative Stress▽

Abhik Sen,[1] Nabendu Sekhar Chatterjee,[2] M. Ali Akbar,[1]† Nilay Nandi,[1] and Pradeep Das[1]*

Division of Microbiology, National Institute of Cholera and Enteric Diseases, P-33, C.I.T. Road, Scheme-XM, Beliaghata, Kolkata-700 010, India,[1] and Division Of Biochemistry, National Institute of Cholera and Enteric Diseases, P-33, C.I.T. Road, Scheme-XM, Beliaghata, Kolkata-700 010, India[2]

Received 27 September 2006/Accepted 5 February 2007

The 29-kDa surface antigen (thiol-dependent peroxidase; Eh29) of *Entamoeba histolytica* exhibits peroxidative and protective antioxidant activities. During tissue invasion, the trophozoites are exposed to oxidative stress and need to deal with highly toxic reactive oxygen species (ROS). In this investigation, attempts have been made to understand the role of the 29-kDa peroxidase gene in parasite survival and pathogenesis. Inhibition of *eh29* gene expression by antisense RNA technology has shown approximately 55% inhibition in *eh29* expression, maximum ROS accumulation, and significantly lower viability in 29-kDa downregulated trophozoites during oxidative stress. The cytopathic and cytotoxic activities were also found to decrease effectively in the 29-kDa downregulated trophozoites. Size of liver abscesses was substantially lower in hamsters inoculated with 29-kDa downregulated trophozoites compared to the normal HM1:IMSS. These findings clearly suggest that the 29-kDa protein of *E. histolytica* has a role in both survival of trophozoites in the presence of ROS and pathogenesis of amoebiasis.

Entamoeba histolytica, the enteric protozoa, is a well-established causative agent of amoebic dysentery and liver abscesses in humans (37). *E. histolytica* is well known for its high potential for invading and destroying human tissue, leading to diseases such as hemorrhagic colitis and extraintestinal abscesses (30). The parasite usually lives and multiplies within the human gut, which constitutes an environment of reduced oxygen pressure. During tissue invasion, *E. histolytica* is exposed to elevated amounts of exogenous reactive oxygen species (ROS), such as superoxide radical anions ($O_2^{\cdot -}$) and hydrogen peroxide (H_2O_2) (14, 26). These highly toxic molecules cause severe damage to biological macromolecules, leading to metabolic malfunctions. In addition, *E. histolytica* has to inactivate the ROS produced by endogenous enzymes for its survival. Several defense mechanisms exist in which a wide array of enzymatic and nonenzymatic antioxidants, including superoxide dismutase (SOD), glutathione peroxidase, catalase, and glutathione, play an active role in cell survival during oxidative stress. *E. histolytica* produces an iron-containing SOD that is induced by superoxide anions to produce H_2O_2 (9). Hydroperoxides produced during oxidative stress could be detoxified by a bifunctional NADPH:flavin oxidoreductase containing NADPH-dependent disulfide reductase and a H_2O_2-forming NADPH oxidase activity (10, 12). Catalase and glutathione reductase systems are absent in *E. histolytica*, but it encodes a 29-kDa cysteine-rich antigen (thiol-dependent peroxiredoxin) located on the surface of the trophozoites (8). The 29-kDa thiol-dependent peroxiredoxin of *E. histolytica* (Eh29) is homologous to AhpC (alkyl hydroperoxide C-22 protein) of *Salmonella enterica* serovar Typhimurium and *Saccharomyces cerevisiae* thiol-specific antioxidant protein (17). In our previous study it was clearly demonstrated that the enzymes SOD and Eh29 increased by 1.7- and 2.1-fold, respectively, in 1-hour high-oxygen-exposed trophozoites compared to controls. This suggests the synchronous involvement of SOD and Eh29 in detoxification of ROS (1) and survival of the parasite under stressed conditions. Thus, it could be said that Eh29 plays an important role in survival of the parasite in highly oxidative environments.

Therefore, the aim of this study was to decrease the expression of Eh29 in *E. histolytica* using an antisense RNA technique and to show that the trophozoites become susceptible to oxidative stress. For antisense RNA inhibition, a series of plasmid vectors both inducible and constitutive has been successfully used to study the in vivo effects of certain genes in *Entamoeba* spp. (2, 3, 6, 19, 21, 24, 32). In this study a cloned fragment of the *E. histolytica eh29* gene was inserted in the antisense orientation in a tetracycline-inducible expression vector (18, 27, 29). Tetracycline-induced transfected trophozoites of *E. histolytica* showed reduced levels of *eh29* mRNA and protein expression. The Eh29-deficient parasites were more sensitive than the wild type to an oxygenated environment as well as H_2O_2 in axenic culture.

* Corresponding author. Present address: Rajendra Memorial Research Institute of Medical Sciences, Agam Kuan, Patna 800 007, India. Phone: 91 612 2636651. Fax: 91 612 2634379. E-mail: drpradeep.das@gmail.com.

† Present address: Southwestern Medical Center, University of Texas, Dallas, TX.

▽ Published ahead of print on 16 February 2007.

MATERIALS AND METHODS

Cultivation and maintenance of *E. histolytica*. Trophozoites of *E. histolytica* strain HM1:IMSS were cultured axenically in TYI-S-33 medium (16), supplemented with 10% heat-inactivated bovine serum and 3% complete vitamin mix at 37°C. Transfected trophozoites were grown in the presence of 5 μg/ml hygro-

mycin. The dose of hygromycin was increased gradually until the growth rates of the transfected trophozoites were similar to that of the control cells.

Construction of plasmid. The tetracycline-controlled gene expression vector pEhHYG-tetR-O-CAT (18, 29) was used as the basic construct for our experiment (kind gift from Egbert Tannich, Bernhard Nocht Institute for Tropical Medicine, Germany) for regulation of the *eh29* gene in *Entamoeba histolytica*. A 422-bp fragment from the 5′ end of the *eh29* gene was amplified using primers AF (5′-GGGGTACCGAATGTCAACTTTCCTACTCC) and AR (5′-CGGGATCCTCAATCAGTCAAATGTCTTGC) by PCR. The PCR conditions used were denaturation for 30 s at 95°C, annealing at 55°C for 30 s, extension at 72°C for 1 min, and a final extension at 72°C for 5 min. The PCR product was inserted into the pEhHYG-tetR-O-CAT vector backbone between KpnI and BamHI restriction sites (underlined). This insertion resulted in placement of *eh29* in a reverse orientation downstream of the lectin promoter, producing the hybrid plasmid pEhHYG-tetR-O-reveh29, which on induction with tetracycline produces the antisense RNA.

Transfection and selection of drug-resistant *E. histolytica* phenotype. Transfection of plasmids in *E. histolytica* was performed by electroporation as described by Purdy et al. (28), with slight modifications under electroporation conditions (3). Briefly, *E. histolytica* trophozoites in logarithmic phase were kept in ice for 5 min, centrifuged at 400 × *g* for 5 min, and washed once in incomplete cytomix buffer (120 mm KCl, 0.15 mM $CaCl_2$, 10 mM K_2HPO_4/KH_2PO_4, pH 7.5, 25 mM HEPES, 2 mM EGTA, 5 mM $MgCl_2$, final pH 7.8 to 7.9). Washed trophozoites were resuspended in 0.8 ml of incomplete cytomix buffer, supplemented with 2 mM ATP and 5 mM glutathione, at a concentration of 1.5×10^7 per ml. Immediately, 2.5 μl of DEAE-dextran (1 mg/ml) was added to the cell suspension and it was transferred to a 0.4-cm electroporation cuvette (Bio-Rad) and incubated with 100 μg purified circular plasmid. Transfections were carried out in a Bio-Rad Gene Pulser II at 1.2-kV voltage, 3,000-V/cm field strength, and 25-μF capacitance with a time constant of 0.4 ms. After transfection, the cuvette was immediately placed on ice for 15 min and trophozoites were transferred to 15-ml sterile screw-cap culture tubes containing 11 ml TYI-S-33 medium. The transfected trophozoites were initially incubated with 5 μg/ml hygromycin, and the dose was gradually increased to 10 μg/ml to obtain stable transfectants. The medium was changed every 24 h with fresh addition of hygromycin.

Selection of tetracycline dose. The control and transfected trophozoites were incubated for 24 h, 48 h, and 72 h with a tetracycline dose of 0.5 μg/ml, 1 μg/ml, and 5 μg/ml (18, 29). Trophozoites were washed once with prewarmed complete TYI-S-33 medium and chilled on ice for 5 min to dislodge the cells from tube surfaces. The viability of the collected trophozoites was examined by trypan blue exclusion (0.5 mg/ml).

Isolation of total RNA. Total RNA was isolated from nontransfected wild-type HM1 trophozoites, transfected control trophozoites (containing pEhHYG-tetR-O-CAT vector only), transfected uninduced trophozoites (pEhHYG-tetR-O-Reveh29), and tetracycline-induced (0.5 μg/ml, 1 μg/ml, and 5 μg/ml) transfected trophozoites (pEhHYG-tetR-O-Reveh29) and from 3-h oxidative stress-induced nontransfected, control transfected, uninduced transfected, and tetracycline-induced transfected trophozoites by using TRIzol reagent (Life Technologies) following the manufacturer's protocol. The quality of RNA was checked by agarose gel electrophoresis and spectrophotometric analysis.

Semiquantitative RT-PCR. Reverse transcription (RT) was performed using 0.2 μg of total RNA and an anchored oligo(dT) (H-dT_{11}M, where M represents A, C, or G nucleotides; GenHunter). The synthesized cDNAs were amplified by PCR, using *eh29* forward and reverse primers. The linear range of the PCR amplification was verified by quantifying the cDNA-PCR product obtained after amplifications for 15 to 30 cycles (data not shown). All PCRs were performed for 25 cycles, which was within the linear range of amplification of the corresponding mRNA species. The products were run on a 1% agarose gel, stained with ethidium bromide, and finally quantitated using Quantity One software (Bio-Rad). All the amplified RT-PCR products were normalized with respect to actin RT-PCR product.

Immunoblot assay. Electrophoretically, 80-μg aliquots of proteins from different transfected trophozoite lysates were resolved in a 10% polyacrylamide gel under reducing conditions and transferred onto a nitrocellulose membrane (Bio-Rad). The membrane was washed with Tris-buffered saline, pH 7.2, blocked with 3% bovine serum albumin (Sigma) at 37°C for 2 h, and reacted with a 1:1,000 dilution of NICED 11 ascites (monoclonal antibody specific for the 29-kDa protein of *E. histolytica*) (33). Fibronectin (1, 34) antibody was used to check the equal loading of proteins. The antigen-antibody reaction was probed with anti-mouse horseradish peroxidase-conjugated immunoglobulin G (Jackson ImmunoResearch). The color reaction was developed with 0.5% diaminobenzedene tetrahydrochloride (Sigma) containing 0.03% H_2O_2.

Detection of reactive oxygen species. Intracellular oxidant levels were determined by the use of 2′,7′-dichlorodihydrofluorescein diacetate (H_2DCF-DA), which is oxidized inside the cell to the fluorescent dichlorofluorescein (DCF). Control and stressed-derived *E. histolytica* trophozoites were incubated with 0.4 mM (final concentration) DCFH-DA for 15 min in the dark. The cells were washed once in phosphate-buffered saline (pH 7.4) and immediately examined under a confocal microscope (LSM510; Zeiss) (1). Measurement was done fluorometrically with excitation at 506 nm and emission at 526 nm (1, 4). The mean fluorescent intensity was analyzed using a Beckman Coulter (Cytomix FC 500) flow cytometer at 530 ± 30 nm. A total of 10,000 cells were analyzed per sample.

Viability assay. Trophozoites in the logarithmic growth phase were washed once with prewarmed complete TYI-S-33 medium and chilled on ice for 5 min to dislodge the cells from tube surfaces. Briefly, 2×10^6 trophozoites in 20 ml complete TYI-S-33 medium were transferred to a 90-mm tissue culture petri dish aseptically and kept at 35°C for different time periods (3 to 5 h). After each hour, culture medium was decanted and the trophozoites were collected. The viability of trophozoites was examined by trypan blue exclusion (0.5 mg/ml).

Measurement of cell viability by MTT assay. Viability of stress-induced cells was determined using an in vitro toxicology assay kit based on 3-(4,5-dimethylthiazole-2-yl)-2,5-diphenyl tetrazolium bromide (MTT) (Sigma). MTT is an organic compound which is converted to the blue formazan salt derivative by the active cellular dehydrogenase of living cells and is measured spectrophotometrically at 570 nm (25). Nontransfected, transfected control, uninduced transfected, tetracycline-induced transfected, and 5 μM catalase-treated tetracycline-induced trophozoites were subjected to oxidative stress for 3 h. The stress-induced cells were incubated with MTT and assayed following the kit protocol.

Assay for membrane integrity. Measurements of the release of the cytosolic enzyme lactate dehydrogenase serve as an indicator of loss of membrane integrity and thus cell viability. In *Entamoeba* the release of pyruvate:ferredoxin oxidoreductase into the culture medium is assayed by incubating samples of culture medium with sodium pyruvate in the presence of NADH. Pyruvate:ferredoxin oxidoreductase present in the culture medium catalyzes the reduction of pyruvate and the concomitant oxidation of NADH to NAD^+. The rate of conversion of NADH to NAD^+ is measured spectrophotometrically at 340 nm (36). Nontransfected, transfected control, uninduced transfected, tetracycline-induced transfected, and 5 μM catalase-treated tetracycline-induced transfected trophozoites were subjected to oxidative stress for 3 h. A 100-μl aliquot of cell medium was collected; 750 μl of NADH (0.3 mg/ml) solution and 150 μl of 20 mM sodium pyruvate were added to it, and activity was measured immediately at 340 nm.

Cell death assay using Annexin V-FLUOS staining kit. Annexin V staining distinguishes apoptotic cells from necrotic cells. To determine the mode of cell death, nontransfected, transfected control, uninduced, tetracycline-induced transfected, and 5 μM catalase-treated tetracycline-induced transfected trophozoites were subjected to 3 h of oxidative stress as described earlier. Normal and stressed derived cells collected after incubation were washed twice in phosphate-buffered saline (pH 7.4) and labeled using the Annexin V-FLUOS staining kit (Roche, Germany) following the manufacturer's protocol. The cells were examined under a confocal microscope (LSM510; Zeiss), and 200 cells were analyzed for each experiment. Cells showing Annexin-positive signal (green fluorescence) are apoptotic cells, and the propidium iodide-positive cells (red signal) are necrotic cells.

Cytopathic activity of trophozoites on cell monolayers. Monolayers of baby hamster kidney (BHK-1) cultured cells were grown in 24-well plates in Dulbecco's modified Eagle's (DME) medium supplemented with 5% fetal calf serum for 60 to 72 h until confluence. A total of 2×10^5 trophozoites (2×10^5/ml suspended in DME medium) were added to the wells containing a BHK-1 cell monolayer (2×10^5/well) washed with serum-free DME medium. Incubation for 1 h was carried out at 37°C in a CO_2 incubator. The reaction was stopped by incubating the plate at 4°C for 10 min, washed with cold saline twice, fixed with 4% formaldehyde for 10 min, and finally washed with cold saline. The cells were then stained with methylene blue (0.1% in borate buffer, 0.1 M, pH 8.7) for 10 min. The excess stain was washed with 0.01 M borate buffer, and the incorporated stain was extracted using HCl (1 ml, 0.1 M) at 37°C for 30 min. The intensity of color was measured at 660 nm (5, 7).

Cytotoxic activity. The cytotoxic activity of viable trophozoites was determined by vital dye exclusion (7, 22). Freshly harvested BHK cells were washed and resuspended in TYI-S-33 medium without serum. The BHK cells were incubated with trophozoites in the ratio 6:1 (9×10^6 BHK cells, 1.5×10^6 trophozoites) at 37°C. Viability was assayed by examining the trypan blue-treated cells in a hemocytometer. The cytotoxic activity was calculated as the percentage of

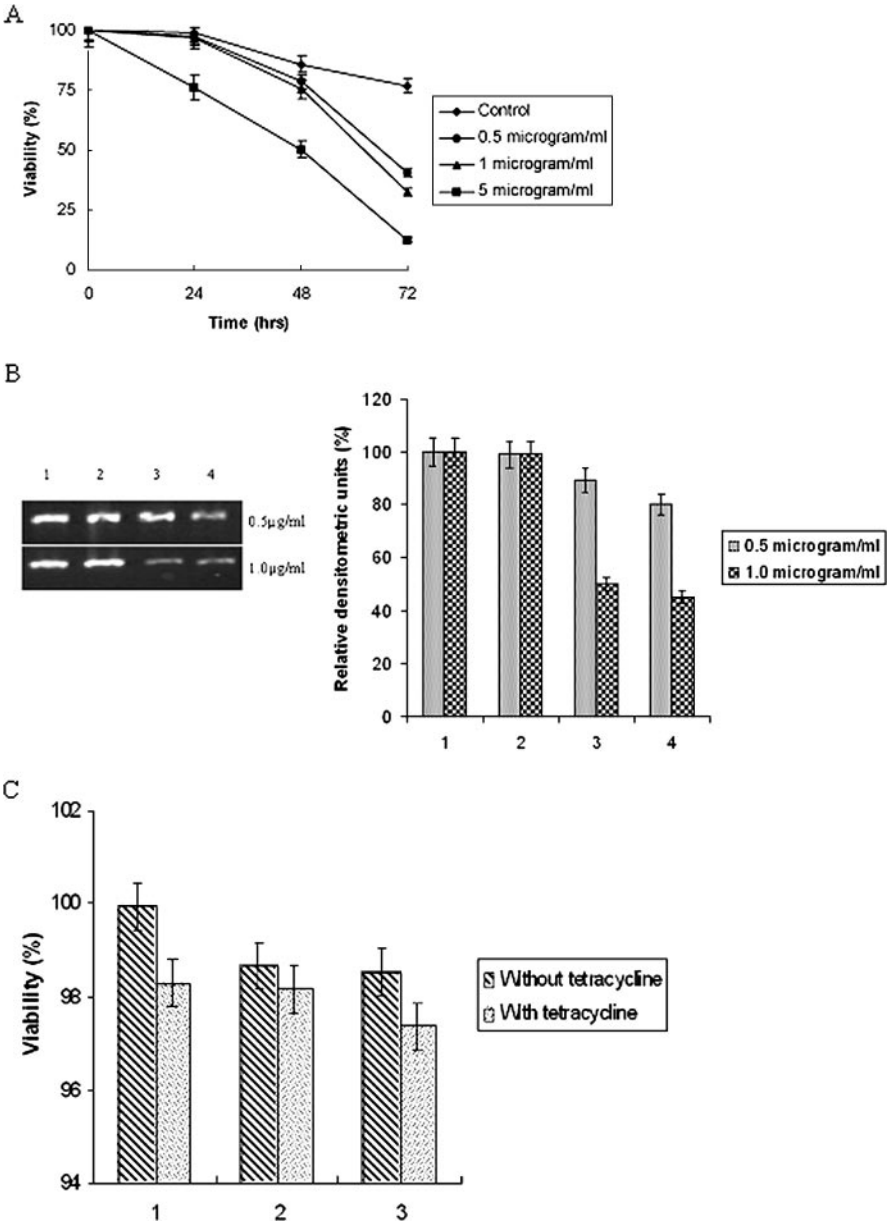

FIG. 1. Tetracycline induction and dose selection. A: Time course viability assay of control and transfected trophozoites for determining the tetracycline dose. Tetracycline at concentrations of 0.5 μg/ml, 1 μg/ml, and 5 μg/ml were added and incubated for 24 h, 48 h and 72 h. B: Semiquantitative RT-PCR analysis for Eh29 expression in 0.5 μg/ml and 1 μg/ml tetracycline-treated trophozoites. The PCR products were separated on (1%) agarose gels and stained with ethidium bromide. Ethidium bromide-stained PCR products were photographed and then images were analyzed densitometrically. PCR products were quantitated and expressed as percentages. Data represent means ± SEM of three independent experiments ($P < 0.05$). Bar sets: 1, nontransfected trophozoites; 2, uninduced pEhHYG-tetR-O-Reveh29-transfected trophozoites; 3, 24-h tetracycline-induced pEhHYG-tetR-O-Reveh29-transfected trophozoites; 4, 48-h tetracycline-induced pEhHYG-tetR-O-Reveh29-transfected trophozoites. C: Viability of control, transfected control, and antisense *eh29*-transfected trophozoites in the presence and absence of 1 μg/ml tetracycline was determined using trypan blue exclusion. Bar sets: 1, nontransfected trophozoites; 2, pEhHYG-tetR-O-CAT-transfected control trophozoites; 3, pEhHYG-tetR-O-Reveh29-transfected trophozoites.

stained cells in the sample minus the percentage of stained cells in the sample with BHK cells alone. The experiment was done in triplicate.

Enzyme assay. The enzymatic activity of alcohol dehydrogenase in the trophozoite lysates from the different types of trophozoites was determined as described previously (23). One unit of activity is defined as 1 μmol of substrate reduced per min per mg of protein.

Ingestion of GFP-labeled *Escherichia coli* cells. *E. coli* cells (1×10^9) containing a plasmid which expresses green fluorescent protein (GFP) were associated in culture medium with different types of trophozoites (1×10^6). The trophozoites with bacteria were harvested after 1 h and washed by centrifugation, and a portion (25%) was fixed with 3.7% formaldehyde. The remaining trophozoites were resuspended in fresh culture medium and were harvested after 24 h, washed, and fixed with formaldehyde. The trophozoites containing fluorescent bacteria were examined under a confocal microscope (7), and the mean fluorescence intensity was measured in a spectrofluorimeter (Perkin-Elmer) at 470-nm excitation and 510-nm emission.

Induction of amoebic liver abscesses. Female Syrian golden hamsters (6 weeks old) were inoculated intrahepatically with 5×10^5 nontransfected, transfected

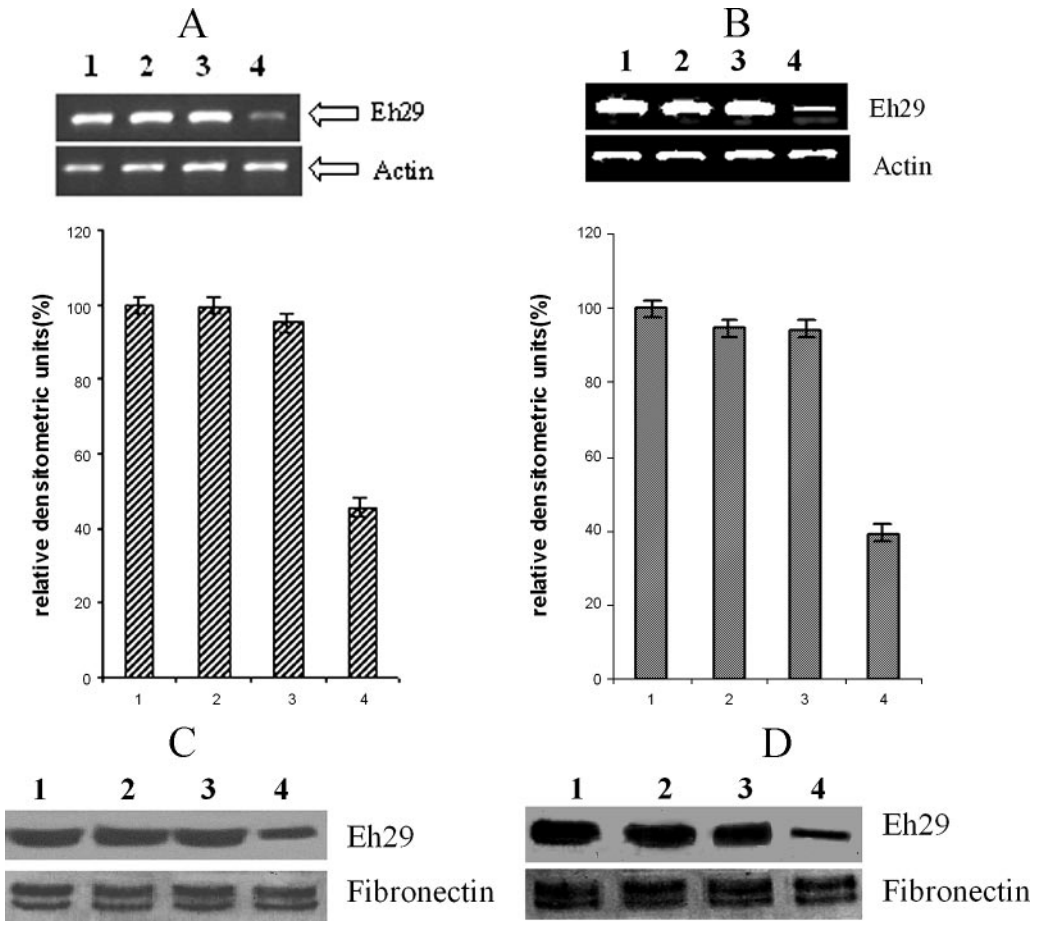

FIG. 2. Expression of the *eh29* gene product in different trophozoites. A and B: Semiquantitative RT-PCR analysis. The PCR products from trophozoites without (A) and with (B) 3-h oxidative stress were separated on a (1%) agarose gel and stained with ethidium bromide. Eh29 and actin products are marked. Ethidium bromide-stained PCR products were photographed and then images were analyzed densitometrically. PCR products were quantitated and expressed as percentages with respect to actin band density. Data represent means ± SEM of three independent experiments ($P < 0.05$). C and D: Immunoblot analysis of the *E. histolytica* 29-kDa protein. The immunoblot was prepared by resolving amoeba lysates from nontransfected and different transfected trophozoites without (C) and with (D) 3-h oxidative stress. The blot was developed with NICED 11 antibody specific for Eh29 and with fibronectin to confirm equal loading of proteins. Data represent means ± SEM of several trophozoites from three independent experiments ($P < 0.05$). Bars: 1, nontransfected trophozoites; 2, pEhHYG-tetR-O-CAT-transfected control trophozoites; 3, uninduced pEhHYG-tetR-O-Reveh29-transfected trophozoites; 4, tetracycline-induced pEhHYG-tetR-O-Reveh29-transfected trophozoites.

control, uninduced transfected, and tetracycline-induced transfected trophozoites. Hamsters (four in each group) were sacrificed 1 week after intrahepatic inoculation, and formation of lesions was evaluated. Hamsters used in this study were approved by the Institutional Review Board, and animal experiments were conducted under appropriate regulatory guidelines.

Statistical analysis. Data are means ± standard errors of the means (SEM) of multiple experiments. Statistical differences were analyzed by one-way analysis of variance, with statistical significance being set at 0.05 ($P < 0.05$).

RESULTS

Dose selection of tetracycline. The viabilities of the transfected and control trophozoites were assayed with increasing doses of tetracycline in a time-dependent manner. A 24-h incubation with a 0.5-μg/ml or 1-μg/ml dose of tetracycline revealed around 97% viability. The viability was significantly decreased with a dose of 5 μg/ml tetracycline when incubated for same time period (Fig. 1A). With an increase in the period of incubation with different doses of tetracycline, the viability of the trophozoites decreased gradually. The viability was significant only with 24-h incubation on exposure to tetracycline doses of 0.5 μg/ml and 1 μg/ml, but the expression of the inserted gene was maximum with a dose of 1 μg/ml when incubated for a period of 24 h (50% downregulation in *eh29* expression) compared to induction with 0.5 μg/ml (11% downregulation). After 48 h of incubation with 1 μg/ml tetracycline, *eh29* expression was downregulated by 55%, while after incubation with 0.5 μg/ml tetracycline the *eh29* expression was downregulated by 20% (Fig. 1B). Therefore, in the experimental procedures the transfected trophozoites were induced with a dose of 1 μg/ml of tetracycline for 24 h to achieve maximal expression of the inserted gene. The viabilities of the control, transfected control, and antisense *eh29* transfected trophozoites in the presence or absence of 1 μg/ml tetracycline were found to be almost similar (Fig. 1C), inferring that 1 μg/ml of tetracycline was not lethal for the parasites.

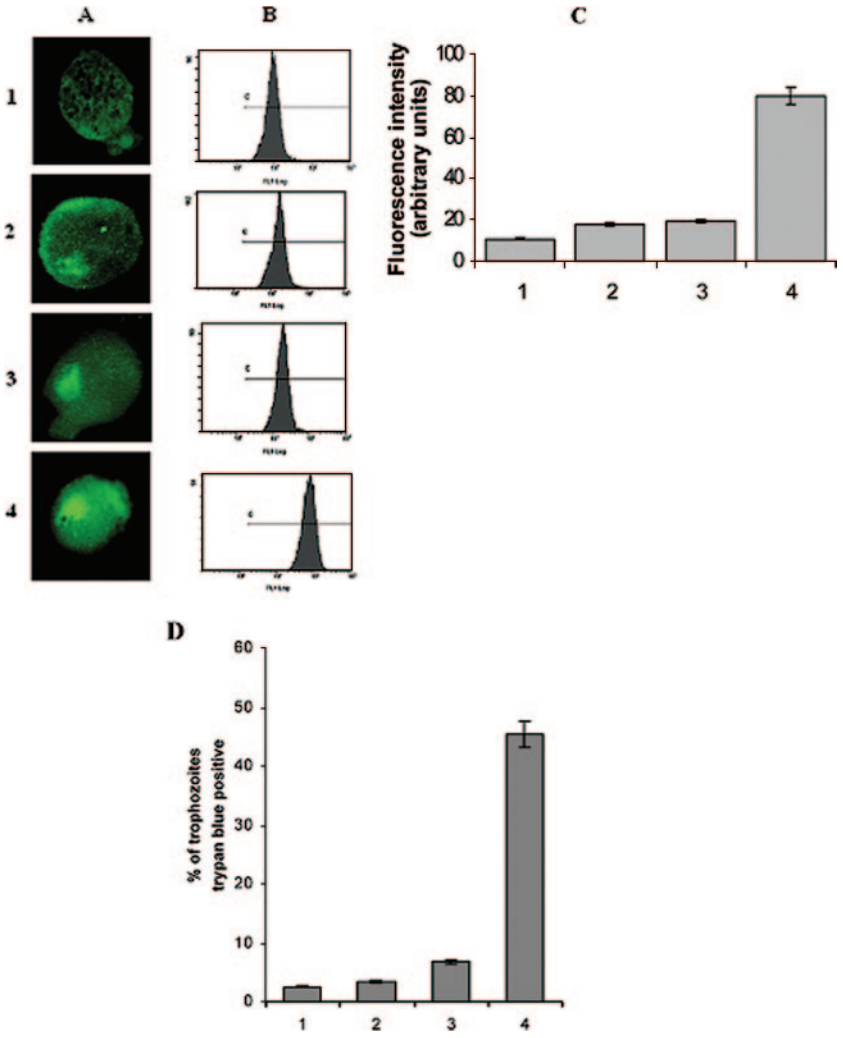

FIG. 3. Generation of reactive oxygen species production and viability analysis of stressed trophozoites. *E. histolytica* trophozoites were subjected to 3 h of oxidative stress, and ROS generation was analyzed by confocal microscopy and flow cytometer using DCFH-DA (see Materials and Methods for details). Viability was examined by trypan blue exclusion. A: Relative expression of ROS in *E. histolytica* trophozoites as viewed under a laser confocal microscope. B: Histogram representing relative expression of ROS as obtained with a flow cytometer. C: Mean fluorescence intensity indicating expression of ROS of the trophozoites. D: Percentage of dead cells. Data represent means ± SEM of three independent experiments ($P < 0.05$). Bars: 1, nontransfected trophozoites; 2, pEhHYG-tetR-O-CAT-transfected control trophozoites; 3, uninduced pEhHYG-tetR-O-Reveh29-transfected trophozoites; 4, tetracycline-induced pEhHYG-tetR-O-Reveh29-transfected trophozoites.

Antisense *eh29* significantly reduces the 29-kDa gene product. The mRNA levels of the *eh29* gene in nontransfected, transfected control (pEhHYG-tetR-O-CAT-containing trophozoites), uninduced transfected trophozoites, and tetracycline-induced transfected trophozoites under normal and stress-inducing conditions were quantified using semiquantitative RT-PCR. The expression level of *eh29* in tetracycline-induced trophozoites was found to be reduced by 55% from control trophozoites. The mRNA levels of *eh29* in nontransfected and transfected control trophozoites were quite similar. No prominent change was noticed in the expression level of actin in the four different types of trophozoites (Fig. 2A). Under 3-h stressed conditions, the downregulation of *eh29* expression in the tetracycline-induced transfected trophozoites was maintained, and it was 60% reduced compared to the control (Fig. 2B).

NICED 11 monoclonal antibody specific for the 29-kDa protein of *E. histolytica* was used in an immunoblot analysis. Identical amounts of protein from nontransfected, control, uninduced transfected, and tetracycline-induced transfected trophozoites revealed a 50% decrease in the 29-kDa protein in tetracycline-induced transfected trophozoites (Fig. 2C). Nontransfected, control, and uninduced trophozoites produced nearly similar amounts of the 29-kDa protein. The same effect was also maintained in the oxidatively stressed trophozoites (Fig. 2D).

Downregulation of Eh29 affects survival of the trophozoites under O_2-stressed conditions. Previously, our group showed that the maximum ROS level accumulated at 3-h, high-oxygen-stressed trophozoites compared to normal trophozoites, and the level increased in the order of 1 h < 2 h < 3 h (1). In the present investigation, it was found that the mean fluorescence

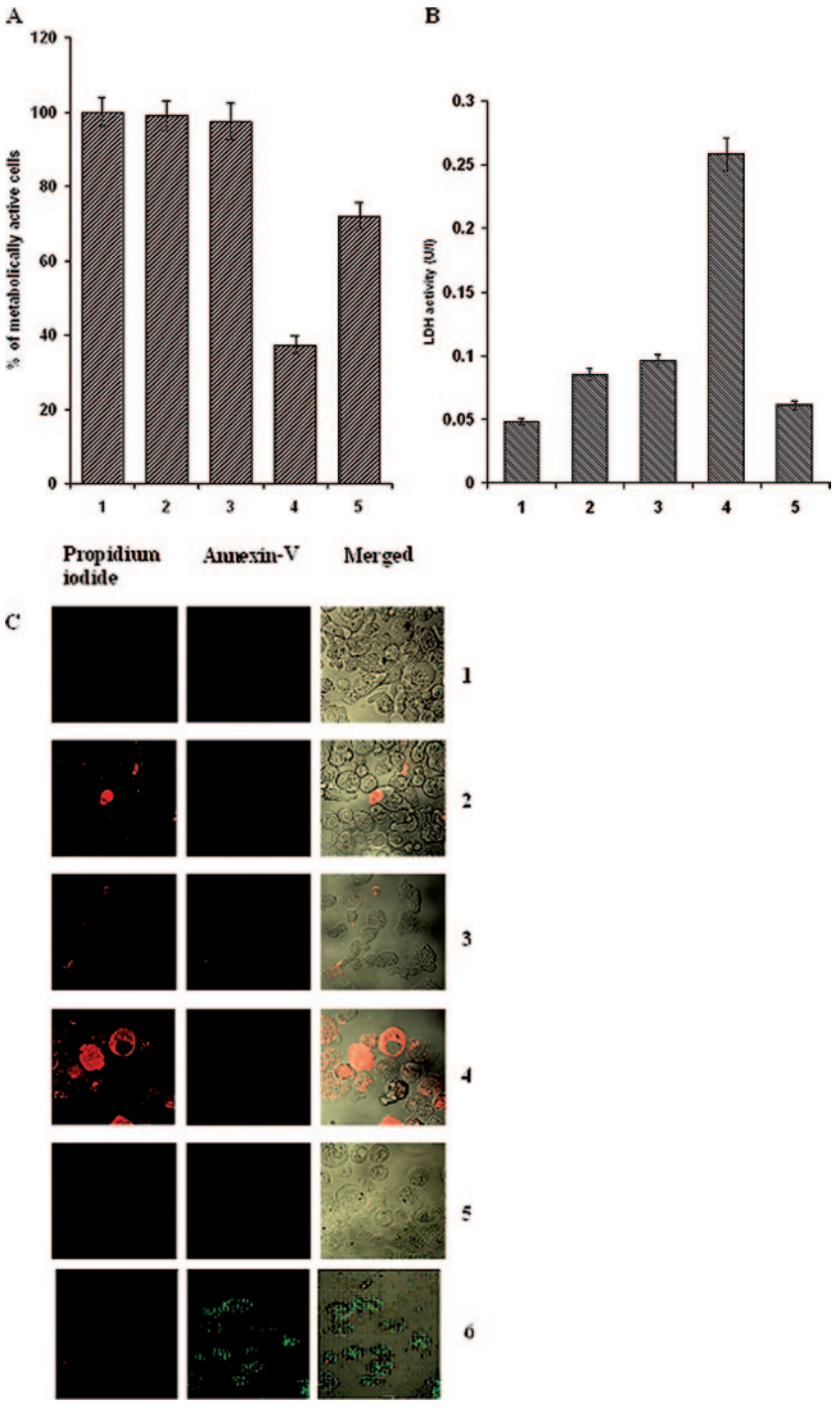

FIG. 4. Effect of antisense *eh29* on physiological activity and death of the trophozoites during oxidative stress. A: Viability assay of stressed trophozoites using MTT (for details, see Materials and Methods). B: Loss of membrane integrity during oxidative stress. Release of the cytosolic enzyme pyruvate:ferredoxin oxidoreductase served as an indicator of loss of membrane integrity and thus cell viability. Bars: 1, nontransfected trophozoites; 2, pEhHYG-tetR-O-CAT-transfected control trophozoites; 3, uninduced pEhHYG-tetR-O-Reveh29-transfected trophozoites; 4, tetracycline-induced pEhHYG-tetR-O-Reveh29-transfected trophozoites; 5, 5 μM catalase-treated tetracycline-induced transfected trophozoites. Data represent means ± SEM of three independent experiments ($P < 0.05$). C: The cell death assay was done using an Annexin V-FLUOS kit. The left column represents propidium iodide-positive trophozoites, the middle column represents Annexin-positive trophozoites, and the right column represents a combined image. Panels: 1, nontransfected trophozoites; 2, pEhHYG-tetR-O-CAT-transfected control trophozoites; 3, uninduced pEhHYG-tetR-O-Reveh29-transfected trophozoites; 4, tetracycline-induced pEhHYG-tetR-O-Reveh29-transfected trophozoites; 5, 5 μM catalase-treated tetracycline-induced transfected trophozoites; 6, nontransfected trophozoites exposed to oxidative stress for 6 h.

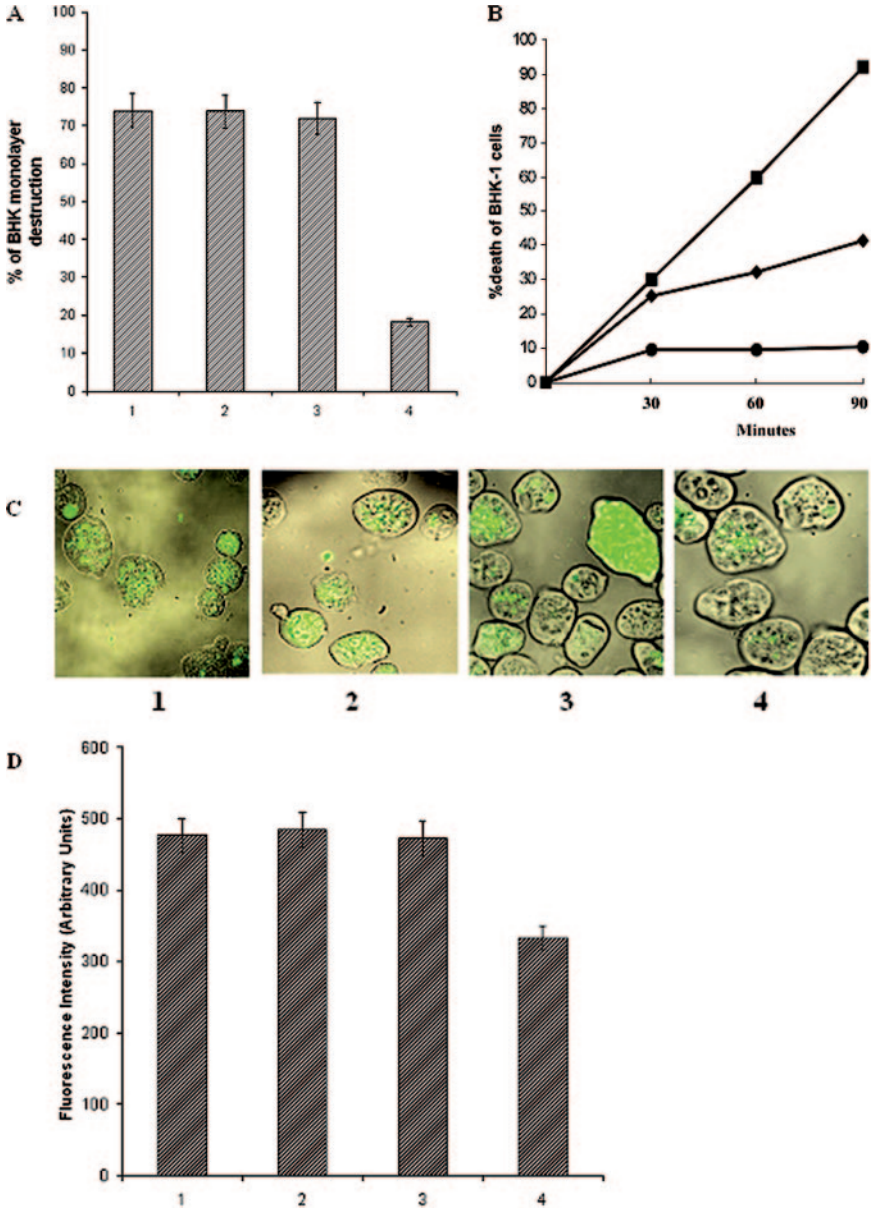

FIG. 5. Pathogenic effects of different trophozoite groups. A: Cytopathic activity of trophozoites. Trophozoites (2×10^5) were incubated with BHK cells. After 1 h of interaction, the destruction of the BHK tissue culture monolayer was determined as described in Materials and Methods. B: Cytotoxic activity of *E. histolytica* trophozoites (1.5×10^6) incubated in suspension with BHK cells (9×10^6). Viability was determined by trypan blue exclusion as described in Materials and Methods. ●, BHK cells alone; ■, nontransfected parent HM1 strain; ◆, tetracycline-induced pEhHYG-tetR-O-Reveh29-transfected trophozoites. C: Confocal fluorescence microscopy of trophozoites that ingested GFP-labeled *E. coli* cells. Trophozoites were associated with the bacteria for 1 h, after which they were harvested and washed. A portion of the total amount of trophozoites was then fixed in formaldehyde, and the image obtained by phase contrast with the fluorescent image shows the bacterial location in the vacuoles. D: Fluorescence intensity emitted by GFP-labeled bacteria phagocytosed by the different trophozoites, as measured in a spectrofluorimeter at 470-nm excitation and 510-nm emission. Panels (C) and bars (D): 1, nontransfected trophozoites; 2, pEhHYG-tetR-O-CAT-transfected control trophozoites; 3, uninduced pEhHYG-tetR-O-Reveh29-transfected trophozoites; 4, tetracycline-induced pEhHYG-tetR-O-Reveh29-transfected trophozoites. Data represent means ± SEM of three independent experiments ($P < 0.05$).

intensity was maximum in tetracycline-induced pEhHYG-tetR-O-Reveh29-containing trophozoites. The comparative analysis in ROS levels demonstrated 1.672-, 1.8-, and 7-fold increases in transfected trophozoites without antisense, transfected trophozoites with antisense, and tetracycline-induced transfected trophozoites with antisense, respectively (Fig. 3A and B).

Survivability of these stressed trophozoites was studied by vital dye exclusion, and it showed that tetracycline-induced pEhHYG-tetR-O-Reveh29-transfected trophozoites were 55% viable, compared to 97.5% in nontransfected trophozoites. The uninduced transfected trophozoites and the transfected control trophozoites showed 93% and 95% viability, respectively, after 3 h of oxidative stress (Fig. 3C).

Downregulation of Eh29 affects physiological activities in trophozoites. An MTT assay of the trophozoites showed that under stressed conditions the tetracycline-induced transfected trophozoites were 62.6% less metabolically active than the nontransfected trophozoites. Catalase-treated cells showed 72% viability. The transfected control trophozoites showed 99% viability, and uninduced transfected trophozoites showed 97.5% viability compared to nontransfected trophozoites (Fig. 4A).

Membrane integrity as determined by the release of pyruvate:ferredoxin oxidoreductase from the cells was found to be significantly less in the tetracycline-induced transfected trophozoites than in the nontransfected, transfected control, and uninduced transfected trophozoites. The pyruvate:ferredoxin oxidoreductase activity was almost five times higher in the induced trophozoites than the control. In catalase-treated trophozoites the pyruvate:ferredoxin oxidoreductase release was quite similar to the nontransfected trophozoites (Fig. 4B).

The cell death assay using the Annexin V-FLUOS staining kit revealed that the mode of cell death due to oxidative stress in the tetracycline-induced transfected trophozoites is necrosis, as nearly 75% of the cells were propidium iodide positive. No significant increases in dead cells were encountered in the nontransfected trophozoites. Two percent of transfected control trophozoites, 3.5% of uninduced transfected trophozoites, and 2.5% of the catalase-treated tetracycline-induced transfected trophozoites gave a propidium iodide-positive signal (Fig. 4C). In the 6-h oxidatively stressed normal cells, Annexin V-positive signal was found.

Antisense Eh29-downregulated trophozoites exhibit decreased cytopathic and cytotoxic effects. A significant decrease in cytopathic activity was observed in the tetracycline-induced transfected trophozoites (>55%) compared to normal HM1:IMSS trophozoites when allowed to interact with a monolayer of BHK cells for 60 min (Fig. 5A). Transfected control trophozoites exhibited cytopathic activity very similar to nontransfected trophozoites of the parent *E. histolytica* strain. The uninduced transfected trophozoites showed cytopathic activity quite similar to nontransfected trophozoites.

The cytotoxic effect of the trophozoites on BHK cells was measured by the damage to the membranes of suspended BHK cells, as detected by trypan blue exclusion. The nontransfected trophozoites showed 92% cytotoxic activity at 90 min compared to 41.6% cytotoxic activity in tetracycline-induced transfected trophozoites (>55% decrease in cytotoxicity) (Fig. 5B). The control transfected trophozoites showed very similar results (85%) as nontransfected trophozoites, and uninduced transfected trophozoites showed 74.6% cytotoxic activity.

Effect of antisense Eh29 on phagocytic ability of trophozoites. A marked decrease in the ingestion of fluorescent-labeled bacteria (Fig. 5C) was noticed in the induced transfected trophozoites (69.7%) (Fig. 5D) compared to the nontransfected, control transfected, and uninduced transfected trophozoites.

Effect of antisense inhibition of Eh29 on liver abscess formation in hamsters. To correlate the decrease in cytopathic effect with the general decrease in virulence, liver abscess formation in hamsters was observed after inoculating the animals intrahepatically with 5×10^5 nontransfected, transfected control, uninduced transfected, and tetracycline-induced transfected trophozoites. Hamsters inoculated with parent HM1:IMSS trophozoites, the control transfected trophozoites, or uninduced transfected trophozoites showed extensive necrotic lesions (>20 mm), while of the four hamsters inoculated with tetracycline-induced transfected trophozoites only two showed minor lesions (<10 mm) (Table 1).

TABLE 1. Induction of liver abscess formation in hamsters[a]

Type of trophozoites	Abscess size (mm)
Nontransfected HM1:IMSS	20–25
pEhHYG-tetR-O-CAT-transfected control	20–22
Uninduced pEhHYG-tetR-O-Reveh29 transfected	17–22
Tetracycline-induced pEhHYG-tetR-O-Reveh29 transfected	6–9

[a] Six-week-old female Syrian Golden hamsters were inoculated with 5×10^5 trophozoites after laparatomy and sacrificed after 7 days. Four animals were inoculated with each type of trophozoites.

DISCUSSION

Earlier, our lab demonstrated that in oxidatively stressed trophozoites, ROS levels increased in a time-dependent manner (3 h > 2 h > 1 h). A 2.1-fold overexpression of the *eh29* gene was noticed in 1-h-stressed trophozoites compared to the control trophozoites. Increased levels of the 29-kDa protein were also noticed in oxidatively stressed trophozoites compared to normal trophozoites in an immunoblot assay against NICED 11 monoclonal antibody (1). These observations clearly suggested a possible role of Eh29 in the survival of the parasite and maintaining the pathogenic effect during invasion in the highly oxygenated environment of the host. Catalase- and glutathione-dependent peroxidase activities are absent in *E. histolytica*, but *E. histolytica* contains a peroxiredoxin on the outer surface of the cell which reduces and detoxifies peroxides and peroxynitrites under oxidatively stressed conditions (11). This protein is reported to localize to the parasite host cell contact and can effectively counteract the free radicals generated by the host cell and facilitates invasion (13). Therefore, it could be predicted or possibly true that Eh29, a membrane-associated peroxiredoxin in nature, takes part in the removal of H_2O_2 formed under stressed conditions and helps in the survival of the parasite. To establish the involvement of Eh29 in survival and removal of ROS from the parasite, an antisense regulation technique to inhibit the expression of the *eh29* gene was used.

In the tetracycline-induced *eh29* antisense transfected trophozoites, the expression of the 29-kDa protein was downregulated by almost 50% (Fig. 2). This downregulation affected the survival rate of the parasite under oxidative stress conditions. In 3-h oxidatively stressed cells, the survival rate of the *eh29* downregulated trophozoites was only 65% compared to 97.5% in normal trophozoites. ROS accumulation in the 29-kDa antisense transfected trophozoites showed a sevenfold increase under stress conditions compared to the control trophozoites, suggesting an involvement of the 29-kDa protein in removal of ROS, particularly H_2O_2. In the Eh29 downregulated trophozoites, cellular physiological activities were impaired and membrane integrity was lost under stressed conditions, but the cells were viable in the presence of catalase (Fig. 4). The above evidence confirmed that when the 29-kDa protein was downregulated in the trophozoites, the H_2O_2 level was high, as the

H_2O_2 formed could not be neutralized by the inhibited peroxidase. It is known that increased H_2O_2 levels alter membrane properties and disrupt membrane-bound proteins significantly, thereby killing the trophozoites. Further, almost all the *eh29* downregulated trophozoites were propidium iodide positive, while no such observation was found in the normal trophozoites subjected to oxidative stress. Normal cells were Annexin V positive only after 6 h of oxidative stress, thus suggesting a possible necrotic death in the downregulated trophozoites. Therefore, the 29-kDa membrane-bound protein removes the toxic ROS during oxidative stress and is an essential factor for parasites survival.

Earlier reports have also shown the involvement of Eh29 in pathogenesis (15, 31). We have also made similar observations (unpublished data). To confirm the role of the 29-kDa protein in pathogenesis, cytopathic and cytotoxic effects on BHK1 cells were studied in Eh29 antisense and control trophozoites. The BHK monolayer destruction was only 20% by the 29-kDa-downregulated trophozoites compared to 75% by the normal HMI. The cytotoxic activity was also significantly lower with the 29-kDa-inhibited trophozoites. The phagocytic capability of 29-kDa-inhibited trophozoites decreased to 69.7%, and liver abscess size in hamsters was significantly lower, confirming the result obtained by Soong et al. (35). All these findings clearly revealed that Eh29 has a definite role in pathogenesis. However, growth culture rates, protein electrophoretic patterns, and basal levels of alcohol dehydrogenase were almost similar in the nontransfected, the transfected control, the uninduced transfected, and the tetracycline-induced transfected trophozoites, inferring that the other functions of the cells are normal and decreased pathogenic effects are only due to downregulation of the 29-kDa protein.

Eh29 is a thiol-specific antioxidant and is a GalNAc lectin-associated protein (20); therefore, it may be concluded that during the host-parasite interface the lectin recruits Eh29 (thiol-specific antioxidant protein), which serves as a mechanism by which the parasite protects itself during tissue adherence and invasion from oxidative attack by the activated host phagocytic and epithelial cells, facilitating invasion.

Thus, in the future the 29-kDa protein can be used as a target for rational drug design for treatment of amoebic liver abscess.

REFERENCES

1. **Akbar, M. A., N. S. Chatterjee, P. Sen, A. Debnath, A. Pal, T. Bera, and P. Das.** 2004. Genes induced by a high oxygen environment in Entamoeba histolytica. Mol. Biochem. Parasitol. **133:**187–196.
2. **Alon, R. N., R. Bracha, and D. Mirelman.** 1997. Inhibition of expression of the lysine-rich 30 kDa surface antigen of *Entamoeba dispar* by the transcription of its antisense RNA. Mol. Biochem. Parasitol. **90:**193–201.
3. **Ankri, S., F. Padilla-Vaca, T. Stolarsky, L. Koole, U. Katz, and D. Mirelman.** 1999. Antisense inhibition of expression of the light subunit (35 kDa) of the Gal/GalNAc lectin complex inhibits *Entamoeba histolytica* virulence. Mol. Microbiol. **33:**327–337.
4. **Bourre, L., S. Thibaut, A. Briffaud, N. Rousset, S. Eleouet, Y. Lajat, and T. Patrice.** 2002. Indirect detection of photosensitizer ex vivo. J. Photochem. Photobiol. B **67:**23–31.
5. **Bracha, R., and D. Mirelman.** 1984. Virulence of *Entamoeba histolytica* trophozoites: effect of bacteria, microaerobic condition, and metronidazole. J. Exp. Med. **160:**353–368.
6. **Bracha, R., Y. Nuchamowitz, M. Leippe, and D. Mirelman.** 1999. Antisense inhibition of amoebapore expression in *Entamoeba histolytica* causes a decrease in amoebic virulence. Mol. Microbiol. **34:**463–472.
7. **Bracha, R., Y. Nuchamowitz, and D. Mirelman.** 2003. Transcriptional silencing of an amoebapore gene in *Entamoeba histolytica*: molecular analysis and effect on pathogenesis. Eukaryot. Cell **2:**295–305.
8. **Bruchhaus, I., and E. Tannich.** 1993. Analysis of the genomic sequence encoding the 29-kDa cysteine-rich protein of *Entamoeba histolytica*. Trop. Med. Parasitol. **44:**116–118.
9. **Bruchhaus, I., and E. Tannich.** 1994. Induction of the iron-containing superoxide dismutase in *Entamoeba histolytica* by a superoxide anion-generating system or by iron chelation. Mol. Biochem. Parasitol. **67:**281–288.
10. **Bruchhaus, I., and E. Tannich.** 1995. Identification of an *Entamoeba histolytica* gene encoding a protein homologous to prokaryotic disulphide oxidoreductases. Mol. Biochem. Parasitol. **70:**187–191.
11. **Bruchhaus, I., S. Richter, and E. Tannich.** 1997. Removal of hydrogen peroxide by the 29 kDa protein of *Entamoeba histolytica*. Biochem. J. **326:** 785–789.
12. **Bruchhaus, I., S. Richter, and E. Tannich.** 1998. Recombinant expression and biochemical characterization of an NADPH:flavin oxidoreductase from *Entamoeba histolytica*. Biochem. J. **330:**1217–1221.
13. **Choi, M. H., D. Sajed, L. Poole, K. Hirata, S. Herdman, B. E. Torian, and S. L. Reed.** 2005. An unusual surface peroxiredoxin protects invasive *Entamoeba histolytica* from oxidant attack. Mol. Biochem. Parasitol. **143:**80–89.
14. **Clark, I. A., N. H. Hunt, and W. B. Cowden.** 1986. Oxygen derived free radicals in the pathogenesis of parasitic diseases. Adv. Parasitol. **25:**1–73.
15. **Davis, P. H., X. Zhang, J. Guo, R. R. Townsend, and S. L. Stanley, Jr.** 2006. Comparative proteomic analysis of two Entamoeba histolytica strains with different virulence phenotypes identifies peroxiredoxin as an important component of amoebic virulence. Mol. Microbiol. **61:**1523–1532.
16. **Diamond, L. S., D. R. Harlow, and C. C. Cunnick.** 1978. A new medium for the axenic cultivation of *Entamoeba histolytica* and other *Entamoeba*. Trans. R. Soc. Trop. Med. Hyg. **72:**431–432.
17. **Flores, B. M., M. A. Batze, M. A. Stein, C. Petersen, D. L. Diedrich, and B. E. Torian.** 1993. Structural analysis and demonstration of the 29-kDa antigen of pathogenic *Entamoeba histolytica* as the major accessible free thiol-containing surface protein. Mol. Microbiol. **7:**755–763.
18. **Hamann, L., H. Buss, and E. Tannich.** 1997. Tetracycline-controlled gene expression in *Entamoeba histolytica*. Mol. Biochem. Parasitol. **84:**83–91.
19. **Hellberg, A., R. Nickel, H. Lotter, E. Tannich, and I. Bruchhaus.** 2001. Overexpression of cysteine proteinase 2 in Entamoeba histolytica or Entamoeba dispar increases amoeba-induced monolayer destruction in vitro but does not augment amoebic liver abscess formation in gerbils. Cell Microbiol. **3:**13–20.
20. **Hughes, M., C. Lee, C. Holm, S. Ghosh, A. Mills, L. A. Lockhart, S. Reed, and B. Mann.** 2003. Identification of *Entamoeba histolytica* thiol-specific antioxidant as a GalNAc lectin-associated protein. Mol. Biochem. Parasitol. **127:**113–120.
21. **Katz, U., R. Bracha, Y. Nuchamowitz, O. Milstein, and D. Mirelman.** 2003. Comparison between constitutive and inducible plasmid vectors used for gene expression in *Entamoeba histolytica*. Mol. Biochem. Parasitol. **128:**229–233.
22. **Leippe, M., J. Andra, and H. J. Müller-Eberhard.** 1994. Cytolytic and antibacterial activity of synthetic peptides derived from amoebapore, the pore forming peptide of E. histolytica. Proc. Natl. Acad. Sci. USA **91:**2602–2606.
23. **Leippe, M.** 1995. Spontaneous release of cysteine proteinases but not of pore-forming peptides by viable Entamoeba histolytica. Parasitology **111:** 569–574.
24. **Moshitch-Moshkovitch, S., R. Petter, A. Levitan, T. Stolarsky, and D. Mirelman.** 1998. Regulation of expression of ribosomal protein L-21 genes of Entamoeba histolytica and E. dispar is at the post-transcriptional level. Mol. Microbiol. **27:**677–685.
25. **Mossman, T.** 1983. Rapid colorimetric assay for cellular growth and survival: application to proliferation and cytotoxicity assays. J. Immunol. Methods **65:**55–63.
26. **Murray, H. W., S. B. Aley, and W. A. Scott.** 1981. Susceptibility of Entamoeba histolytica to oxygen intermediates. Mol. Biochem. Parasitol. **3:**381–391.
27. **Nickel, R., and E. Tannich.** 1994. Transfection and transient expression of chloramphenicol acetyltransferase gene in the protozoan parasite Entamoeba histolytica. Proc. Natl. Acad. Sci. USA **91:**7095–7098.
28. **Purdy, J. E., B. J. Mann, L. T. Pho, and W. A. Petri, Jr.** 1994. Transient transfection of the enteric parasite Entamoeba histolytica and expression of firefly luciferase. Proc. Natl. Acad. Sci. USA **91:**7099–7103.
29. **Ramakrishnan, G., R. R. Vines, B. J. Mann, and W. A. Petri, Jr.** 1997. A tetracycline-inducible gene expression system in Entamoeba histolytica. Mol. Biochem. Parasitol. **84:**93–100.
30. **Ravdin, J. I.** 1988. Human infection by Entamoeba histolytica, p. 166–176. *In* J. I. Ravdin (ed.), Amoebiasis: human infection. John Wiley, New York, NY.
31. **Reed, S. L., B. M. Flores, M. A. Batzer, M. A. Stein, V. L. Stroeher, J. E. Carlton, D. L. Diedrich, and B. E. Torian.** 1992. Molecular and cellular characterization of the 29-kilodalton peripheral membrane protein of *Entamoeba histolytica*: differentiation between pathogenic and nonpathogenic isolates. Infect. Immun. **60:**542–549.
32. **Sahoo, N., S. Bhattacharya, and A. Bhattacharya.** 2003. Blocking the expression of a calcium binding protein of the protozoan parasite Entamoeba histolytica by tetracycline regulatable antisense-RNA. Mol. Biochem. Parasitol. **126:**281–284.

33. **Sengupta, K., P. Das, T. M. Johnson, P. P. Chaudhuri, D. Das, and G. B. Nair.** 1993. Production and characterization of monoclonal antibodies against a highly immunogenic fraction of Entamoeba histolytica (NIH:200) and their application in the detection of current amoebic infection. J. Eukaryot. Microbiol. **40:**722–726.
34. **Sengupta, K., V. I. Hernandez-Ramirez, A. Rios, R. Mondragon, and P. Talamas-Rohana.** 2001. Entamoeba histolytica: monoclonal antibody against the β1 integrin-like molecule (140 kDa) inhibits cell adhesion to extracellular matrix components. Exp. Parasitol. **98:**83–89.
35. **Soong, C. J., B. E. Torian, M. D. Abd-Alla, T. F. Jackson, V. Gatharim, and J. I. Ravdin.** 1995. Protection of gerbils from amebic liver abscess by immunization with recombinant *Entamoeba histolytica* 29-kilodalton antigen. Infect. Immun. **63:**472–477.
36. **Wagner, A., A. Marc, and J. M. Engasser.** 1992. The use of lactate dehydrogenase (LDH) release kinetics for the evaluation of death and growth of mammalian cells in perfusion reactors. Biotechnol. Bioeng. **39:**320–326.
37. **World Health Organization.** 1998. The World Health Report 1998. Life in the 21st century: a vision for all. World Health Organization, Geneva, Switzerland.